The Varied Impacts of El Niñ o–Southern Oscillation on Pacific Island Climates

3 authors:

Bradley F. Murphy
Bureau of Meteorology
21 PUBLICATIONS   1,111 CITATIONS

SEE PROFILE

Scott Power
Bureau of Meteorology
128 PUBLICATIONS   9,287 CITATIONS

SEE PROFILE

Simon Mcgree
Bureau of Meteorology
23 PUBLICATIONS   453 CITATIONS

SEE PROFILE

Some of the authors of this publication are also working on these related projects:

Pacific Climate Change Science Program View project

ENSO & climate change View project

The Varied Impacts of El Niño–Southern Oscillation on Pacific Island Climates

BRADLEY F. MURPHY AND SCOTT B. POWER

Centre for Australian Weather and Climate Research, Bureau of Meteorology, Melbourne, Victoria, Australia

SIMON MCGREE

National Climate Centre, Bureau of Meteorology, Melbourne, Victoria, Australia

ABSTRACT

El Niño–Southern Oscillation (ENSO) drives interannual climate variability in many tropical Pacific island countries, but different El Niño events might be expected to produce varying rainfall impacts. To investigate these possible variations, El Niño events were divided into three categories based on where the largest September–February sea surface temperature (SST) anomalies occur: warm pool El Niño (WPE), cold tongue El Niño (CTE), and mixed El Niño (ME), between the other two.

Large-scale SST and wind patterns for each type of El Niño show distinct and significant differences, as well as shifts in rainfall patterns in the main convergence zones. As a result, November to April rainfall in many Pacific island countries is significantly different among the El Niño types. In western equatorial Pacific islands, CTE events are associated with drier than normal conditions whereas ME and WPE events are associated with significantly wetter than normal conditions. This is due to the South Pacific convergence zone and intertropical convergence zone moving equatorward and merging in CTE events. Rainfall in the convergence zones is enhanced during ME and WPE and the displacement is smaller. La Niña events also show robust impacts that most closely mirror those of ME events.

In the northwest and southwest Pacific strong CTE events have much larger impacts on rainfall than ME and WPE, as SST anomalies and correspondingly large-scale surface wind and rainfall changes are largest in CTE. While variations in rainfall exist between different types of El Niño and the significant impacts on Pacific countries of each event are different, the two extreme CTE events have produced the most atypical impacts.

1. Introduction

El Niño–Southern Oscillation (ENSO) is the largest source of internally generated climate variability in many regions, particularly on interannual time scales (McPhaden et al. 2006; Collins et al. 2011). Its extreme phases (El Niño and La Niña) are accompanied by major changes in equatorial Pacific sea surface temperatures (SST), Pacific trade winds, and the Walker circulation, thereby producing shifts and changes in intensity of surface wind convergence, convection, and rainfall in the region (Folland et al. 2002), as well as atmospheric temperatures regionally (Power et al. 1998) and global mean temperature (Hoerling et al. 2008). It also

has major teleconnections more remotely (Ropelewski and Halpert 1989; Allan et al. 1996).

ENSO most directly affects climate variability in countries throughout the tropical Pacific region, and accounts for much of the interannual variability in station records on Pacific islands (Collins et al. 2011). Seasonal rainfall patterns in countries to the north of the equator are driven to a large extent by the intertropical convergence zone (ITCZ). The position and intensity of the ITCZ varies interannually with ENSO extremes (Collins et al. 2011). Likewise, countries in the southwest Pacific experience a climate that is heavily influenced by the mean position and seasonal cycle of the position, intensity, and extent of the South Pacific convergence zone (SPCZ; Trenberth 1976; Vincent 1994). The SPCZ shifts substantially in response to the changes in SST gradients and position of surface wind convergence that accompany ENSO variations (Folland et al.

Corresponding author address: Bradley F. Murphy, GPO Box 1289, Melbourne VIC 3001, Australia.
E-mail: b.murphy@bom.gov.au

2002; Vincent et al. 2011; Brown et al. 2011), and changes in its position affect the mean and extreme rainfall in southwest Pacific countries (Griffiths et al. 2003). Seasonal rainfall variability in the western extremity of the Pacific is strongly influenced by the west Pacific monsoon, whose strength, timing, and extent are also affected by the phase of ENSO, particularly by ENSO-related variations in the trade winds (Collins et al. 2011).

The main "center of action" of ENSO SST was, until recently, considered to only occur in the eastern half of the Pacific basin (Philander 1990). This "canonical" El Niño has distinct remote impacts, such as elevated risk of drought in eastern Australia (McBride and Nicholls 1983) and a less active Atlantic hurricane season (Gray 1979). More recently El Niño events have been found to exhibit different "flavors" in the structure of their SST changes, such as El Niño Modoki (Ashok et al. 2007). Recent work (e.g., Kao and Yu 2009; Kug et al. 2009) has shown that El Niño has at least two distinct types; the eastern Pacific El Niño (EPE) has largest SST variations around 150°–90°W (the Niño-3 region) and the central Pacific El Niño (CPE) has its largest SST variations farther west, around 160°E to 150°W (the Niño-4 region). EPE is dominated by thermocline variations whereas CPE is driven more by wind-forced zonal SST advection (Kug et al. 2009). Some studies consider these two processes to represent two distinct modes of ENSO variability. Others, such as Kug et al. (2009), consider there to be a continuum of El Niño with varying relative contributions, and hence posit EPE, CPE, and "mixed" El Niño. The various studies into these variations have used different definitions and terminologies. For example, CPE has also been described as "Dateline El Niño" (Larkin and Harrison 2005) and "warm pool El Niño" (Kug et al. 2009), and the related "El Niño Modoki" (Ashok et al. 2007). EPE has also been named "canonical" or "cold tongue" El Niño (Kug et al. 2009).

The CPE has occurred more often in recent decades, whereas the EPE appeared less frequently (e.g., Yeh et al. 2009). This would be expected with changes in the background mean state caused by global warming (Lee and McPhaden 2010; Kug et al. 2010), but more frequent CPE is also possible due to natural decadal climate variability alone (McPhaden et al. 2011; Yeh et al. 2011). In the two recorded occurrences of EPE in the era of satellite observations since 1979, in 1982/83 and 1997/98, the SPCZ moved very far to the east and north (by as much as 20° northward in the east Pacific) and merged with the ITCZ close to the equator; these are called "asymmetric" or "zonal" SPCZ events as the SPCZ lies parallel to the equator (Vincent et al. 2011). It is suggested that these extreme SPCZ responses to ENSO will become more common in the future with global warming (Cai et al. 2012).

Thus, while the EPE has occurred less frequently in recent times, some of its impacts, especially in rainfall, are potentially much greater or unusual in many Pacific countries due to the extreme changes in the position and intensity of the SPCZ and the ITCZ. This paper examines the impacts of different types of El Niño events in Pacific island countries that experience high interannual climate variability. The main objective is to determine whether the climate impacts in Pacific islands in association with El Niño events vary significantly with different El Niño types, and if so to explain them. Section 2 describes the datasets used and the methods employed for categorizing ENSO events. In section 3 we describe the different types of El Niño events that occur and the features they exhibit. Rainfall variability associated with these events is examined in section 4 at several sites in Pacific island countries in order to investigate the occurrence, or otherwise, of extreme or unusual impacts. Section 5 assesses the relative strengths of the impacts of these different types of events in 15 countries in the region and stations therein. A discussion and summary of results follows in section 6.

2. Data and methods

In this section we describe the datasets used in this study and the method used to categorize El Niño and La Niña events. Station observations from many Pacific islands will show local-scale ENSO impacts in the islands; these are compared with changes evident in various gridded analysis data to link local-scale impacts with larger-scale ocean and atmosphere variability.

A major effort has been undertaken to collect and quality check data from Pacific island and East Timor observing stations under the Pacific Climate Change Science Program and the Pacific–Australia Climate Change Science and Adaptation Planning Program (Power et al. 2011). With close collaboration and invaluable cooperation from the national meteorological services in the 15 partner countries, the aim of this work was to develop the highest-quality and most complete climate record possible.

Station data are available for 15 countries across the Pacific region. Figure 1 is a map showing these countries, which can be regarded as lying in four distinct climatic regions: the western Pacific region (WP) comprising East Timor, Papua New Guinea (PNG), and the Solomon Islands; the tropical northwestern Pacific region (NWP) comprising Palau, the Federated States of Micronesia (FSM), and the Marshall Islands; the equatorial Pacific region (EP) including Nauru, Kiribati, and Tuvalu; and
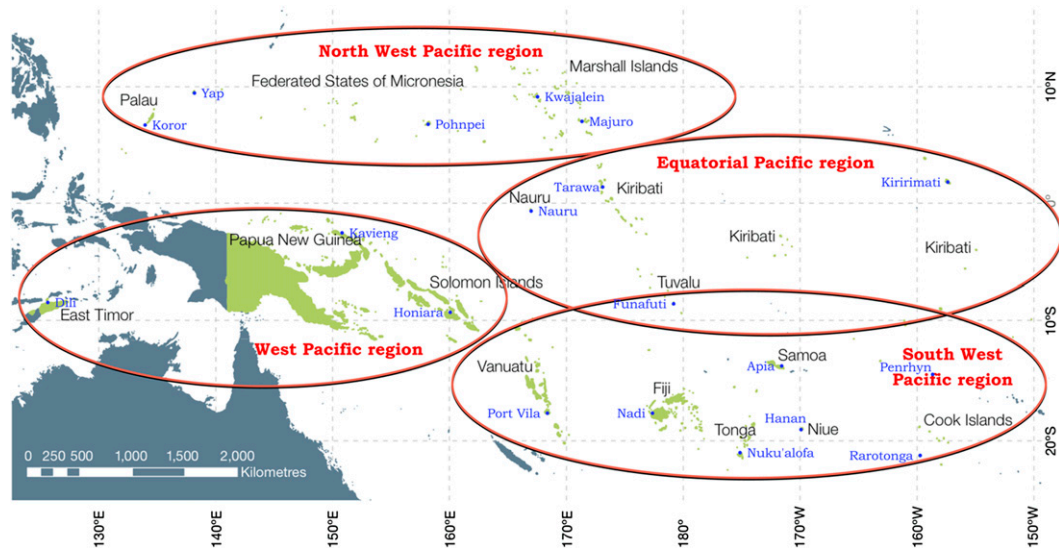
FIG. 1. Map showing the 15 Pacific island countries and East Timor examined. Stations listed in Table 1 are marked in blue. The approximate areas of the four climatic regions discussed in the text are also indicated (after Cambers et al. 2011).

the southwest Pacific region (SWP) that includes Vanuatu, Fiji, Samoa, Niue, Tonga, and the Cook Islands. Table 1 lists the countries considered and the stations used therein, their position, length of record, and number of missing years (several stations have significant data gaps). Monthly rainfall (RR) station data are used. These data have kindly been made available by the meteorological agencies in the countries.

The stations chosen are thought to have the best records in each country. They have been tested for temporal inhomogeneities and corrected for these when necessary (see Murphy et al. 2011; Jones et al. 2012). In most countries one station has been chosen (generally the capital city) to represent the climate, which is relatively homogenous over the smaller countries with no significant topography. Two stations are used in the

TABLE 1. Stations with rainfall data used. Listed are station names and the geographical region in which they lie, their longitude and latitude, the first year, the total number of years with complete data from November to April, and the mean and standard deviations (σ) of total November to April rainfall (RR) in mm.

Country	Station	Lon.	Lat.	First year	Total years	Mean RR Nov–Apr	σ RR Nov–Apr
East Timor	Dili	125.57°E	8.57°S	1952	61	720	205
Papua New Guinea	Kavieng	150.82°E	2.57°S	1918	96	1761	369
Solomon Islands	Honiara	159.97°E	9.42°S	1949	64	1403	421
Vanuatu	Port Vila	168.32°E	17.74°S	1906	106	1417	382
Fiji	Nadi	177.45°E	17.75°S	1942	70	1459	464
Samoa	Apia	171.78°W	13.80°S	1890	123	2030	492
Niue	Hanan	169.93°W	19.08°S	1905	108	1403	416
Tonga	Nuku-alofa	175.18°W	21.13°S	1938	75	1072	366
Cook Islands	Rarotonga (south)	159.80°W	21.20°S	1899	114	1242	312
	Penrhyn (north)	158.05°W	9.03°S	1937	76	1259	709
Tuvalu	Funafuti	179.22°E	8.52°S	1927	86	2022	498
Nauru	Nauru	166.92°E	0.52°S	1927	87	1272	753
Kiribati	Tarawa	172.92°E	1.35°N	1947	66	1186	727
	Kiritmati (Line Islands)	157.48°W	1.98°N	1946	67	610	593
Palau	Koror	134.48°E	7.33°N	1947	67	1563	374
Federated States of Micronesia	Yap (west)	138.08°E	9.48°N	1951	63	1153	378
	Pohnpei (east)	158.22°E	6.97°N	1949	65	2218	496
Marshall Islands	Kwajalein (north)	167.73°E	8.73°N	1945	69	970	304
	Majuro (south)	171.38°E	7.08°N	1954	60	1498	401

Cook Islands, Kiribati, the Marshall Islands, and the Federated States of Micronesia to capture climate variations due to the large areas the islands cover. In PNG, the climate of the capital, Port Moresby, is complicated by surrounding topography, while in Fiji, Suva is exposed to almost constant trade winds so they are thought to not exhibit clear ENSO variability (Cambers et al. 2011); therefore alternative stations were used (Kavieng and Nadi, respectively).

Gridded analysis products across the region used were version 1.1 of the Hadley Centre Sea Ice and Sea Surface Temperature dataset (HadISST) for SST (Rayner et al. 2003), at 1° resolution over the period 1950–2011; version 2.2 of the Global Precipitation Climatology Project (GPCP) rainfall dataset (Adler et al. 2003) at 2.5° resolution from 1979 to 2011; and the Interim European Centre for Medium-Range Weather Forecasts (ECMWF) Re-Analysis (ERA-Interim) surface wind dataset (Dee et al. 2011) interpolated to 1.5° resolution from 1979 to 2011. When calculating anomalies, the standard 1961–90 period is used for the mean climate, except in the GPCP and ERA-Interim data, where the entire 1979–2011 period is used.

The ENSO seasonal cycle tends to peak in December, with El Niño events generally active from around July to March of the following year (e.g., Power and Smith 2007). To cover the main part this cycle we consider a single El Niño or La Niña event over the 6-month period from September to February. Most countries in this region have distinct wet and dry seasons, with all but those in the NWP region having wet seasons from around November to April. There is often a lag between the onset of an ENSO event and the response in rainfall in these countries (Collins et al. 2011). Some countries in the Northern Hemisphere have wet seasons from December to May or May to October, but these seasons either occur before the onset of significant ENSO events or span more than one ENSO cycle. Therefore, the analysis hereafter defines El Niño and La Niña events over the period from September to February, whereas rainfall impacts over countries in the region are averaged from November to April.

ENSO is monitored using the three SST-area average indices Niño-3 (150°–90°W), Niño-3.4 (170°–120°W), and Niño-4 (160°E–150°W), all over 5°S–5°N. We consider an El Niño year to be one in which the September–February mean of any of these three Niño indices exceeds the 1950–2011 standard deviation (σ) of this six-month mean. Similarly, a La Niña year is assigned if one of these indices is $< -\sigma$. This definition is similar to that of Kug et al. (2009, hereafter KUG09), with the exception that our method formalizes the definition of the mixed El Niño type. See the appendix for details of the method and comparison with that of KUG09. It produces very similar

lists of El Niño and La Niña years to other studies using different approaches [e.g., Power and Smith (2007), who used the Southern Oscillation index].

3. Different El Niño types and their impacts

a. El Niño types and SST characteristics

Some El Niño events have their largest SST anomalies in the eastern equatorial Pacific, while others have them in the central Pacific. An effective way of differentiating them is to consider in which of the three equatorial Niño regions the largest SST anomalies occur (similar to KUG09). This region of largest anomaly is therefore used to classify El Niño events into three different types. We use the nomenclature of KUG09: warm pool El Niño (WPE; Niño-4 anomaly largest), mixed El Niño (ME; Niño-3.4 largest), and cold tongue El Niño (CTE; Niño-3 largest). This provides a means of testing if the climate impacts in Pacific islands vary between these El Niño types. The classification first determines if any of the Niño indices exceeds one standard deviation and, if so, the El Niño event is classified according to which index is largest and also exceeds its standard deviation; similarly for La Niña events. KUG09's classification had WPE events where Niño-4 was strongest, CTE events when Niño-3 is strongest, and ME when "maximum SST anomalies are located between 120° and 150°W." The difference between our method and that of KUG09 is that we have formalized the ME definition and have used Niño-3.4 (which is between 170° and 120°W). The results will show that when Niño-3.4 is the strongest of the indices, Niño-3 and Niño-4 are of comparable strengths.

The indices have not been detrended in this analysis. While SST has increased, reflecting global warming trends (Trenberth et al. 2007), the high variability of SST in the equatorial Pacific (interannual standard deviation around 1°C) relative to SST trends (around 0.1°C decade^{-1}) mean linear trends of SST are highly sensitive to the dominant ENSO phase and therefore to the exact dates chosen. Our results are mostly insensitive to detrending, with the only difference being that 1977 and 2006 (the two weakest WPE events) are removed if the data are detrended from 1950 to 2010. Most of our analysis is restricted to the 1979–2011 period when SST data are of high quality; the quality of SST data in the presatellite era may not be high enough to accurately differentiate the different El Niño types (see Tokinaga et al. 2012). High-quality precipitation (GPCP) and wind (ERA-Interim) data are also only available from 1979 to 2011 to conduct analysis of ENSO impacts and teleconnections. The classification therefore only covers 1979–2011; we extend this in section 5 when considering station data.

TABLE 2. Classification from 1979 to 2010 of the three different El Niño types and La Niña, showing the years of events and the mean September–February Niño-4, Niño-3.4, and Niño-4 anomalies for each event, the average of each index for the four types of event, and the standard deviation (σ) of each index.

Type	Year	Niño-4	Niño-3.4	Niño-3
Warm pool El Niño	1994/95	1.01	0.98	0.71
	2004/05	0.90	0.64	0.40
	2006/07	0.79	0.75	0.77
	Average	0.90	0.79	0.63
Mixed El Niño	1986/87	0.79	1.04	0.86
	1987/88	0.98	1.10	1.02
	1991/92	0.86	1.24	1.02
	2002/03	0.94	1.12	0.89
	2009/10	1.21	1.31	1.08
	Average	0.96	1.16	0.97
Cold tongue El Niño	1982/83	0.84	2.14	2.62
	1997/98	1.04	2.35	3.08
	Average	0.94	2.24	2.85
La Niña	1988/89	−1.30	−1.77	−1.43
	1998/89	−0.99	−1.23	−0.69
	1999/2000	−0.92	−1.31	−1.23
	2007/08	−0.88	−1.47	−1.43
	2010/11	−1.13	−1.51	−1.32
	Average	−1.05	−1.46	−1.22
σ Sep–Feb		0.69	0.95	0.95

Table 2 shows the list of resulting El Niño and La Niña events, with the years indicating the start and end of the event. The three El Niño types (determined by which Niño anomaly is greatest) are separated. As can be seen in Table 2, from 1979 to 2011 there have been three WPE, five ME, only two CTE, and five La Niña events. This was evidently a period dominated by El Niño events, although toward the end of the period more La Niña events were observed. This has manifested as interdecadal climate variability in various climate features (e.g., Power and Smith 2007; Power and Kociuba 2012). Updated through to 2010/11, the list of years in this period is very similar to that of KUG09, with the exception of 2002, which we find to be an ME rather than a WPE, and we find that 1990 does not meet any El Niño criteria. The slight differences may also be due to the different SST dataset and time period used by KUG09, which would have different climatological means and standard deviations. A comparison of the methods and their results is provided in the appendix.

There have been only two CTE events since 1979: 1982/83 and 1997/98. These CTE events have much stronger SST anomalies than the other El Niño types and also of La Niña events. This suggests that SST variations due to thermocline variations in the eastern Pacific can be considerably larger than SST changes driven by zonal advection in the west. This is true of the Niño-3 anomalies for these events, but also for Niño-3.4 and

Niño-4 (i.e., the SST anomalies for CTE are stronger across the three regions than for the other types). Also, for ME the Niño-4 anomalies tend to be stronger than for WPE. Indeed, all ME events also qualify as WPE events (and three of them as CTE) except that the Niño-3.4 index is strongest, and similarly all CTE also reach ME and WPE thresholds in the relevant indices. Were they to be classified, all La Niña events would be of mixed type. Other studies have found more than one mode of La Niña SST variability (e.g., Cai and Cowan 2009) but that is not reflected in the current analysis, hence the use of only one La Niña type hereafter.

In the following analysis we investigate the structure of the atmospheric and ocean surface response to these three El Niño types and La Niña, but it is noted here that there is a clear difference in the strengths of the SST anomalies among the types.

The mean September–February SST anomaly patterns for the three El Niño types and La Niña (i.e., the mean anomaly across all years in each category) are shown in Fig. 2. As expected, the maximum anomalies are in the eastern Pacific for CTE, the central Pacific for ME, and western Pacific for WPE. The strength and the areal extent of the anomalies become smaller as the types move from east to west. La Niña events show SST anomalies that most closely mirror the ME, although they tend to be slightly larger in magnitude, particularly in the Niño-3.4 region. Both the CTE and La Niña SST anomaly patterns show extensive regions where the anomalies are statistically significantly different from zero. These cover most of the large equatorial/eastern Pacific area of the positive El Niño (negative La Niña) anomaly and the opposite horseshoe-shaped anomaly to the west. For ME much of the positive anomaly region is also significant, but for WPE only the portion of the positive anomaly close to the date line is statistically significant. Both ME and WPE negative anomaly regions in the west are smaller in magnitude and statistically significant only over very small areas.

Overall, CTE and La Niña clearly have the strongest and most robust SST anomalies. Among the El Niño types CTE has a SST anomaly pattern quite different from the others, while ME and WPE differ less from each other. The main difference between ME and WPE is that outside the Niño-4 region the anomalies are stronger in ME and the area of statistically significant anomalies is much larger. The small area of significant SST anomalies for WPE is most likely due to the relatively small Niño-4 values compared to the respective indices for the other types.

Figure 3 shows the mean monthly cycle of Niño indices for each type of event, from January of the preceding year (Year −1) through the year in which the
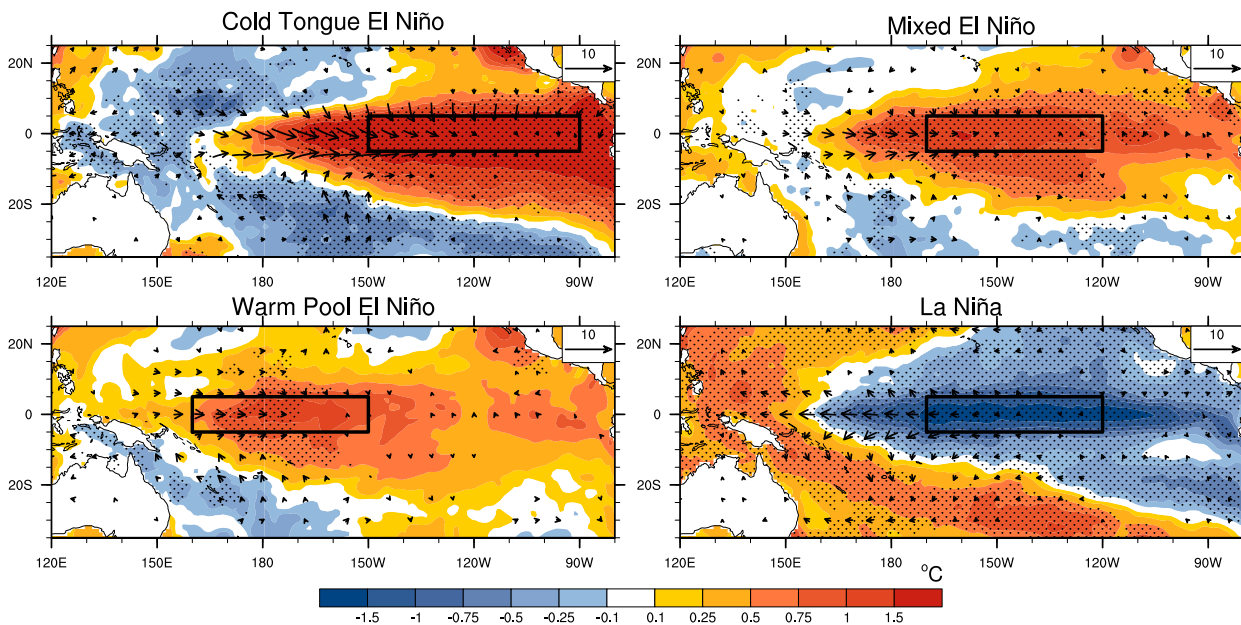
FIG. 2. Mean September–February SST anomalies for the three El Niño types and for La Niña events. Arrows show the corresponding total surface winds, with the reference arrow denoting $10\,\mathrm{m\,s^{-1}}$. Stippling denotes where the SST anomalies are statistically significantly different from zero at the 90% confidence level, and only wind anomalies greater than $5\,\mathrm{m\,s^{-1}}$ are shown.

event peaks (Year 0), and through to December of the following year (Year +1). The index shown for each type is that which is strongest as per the definitions above (Niño-3.4 for La Niña events). All El Niño types

peak around December, whereas La Niña events tend to peak in January. ME and CTE Niño anomalies begin to show warming from around March of Year 0. In contrast, WPE reach a peak SST anomaly in November of
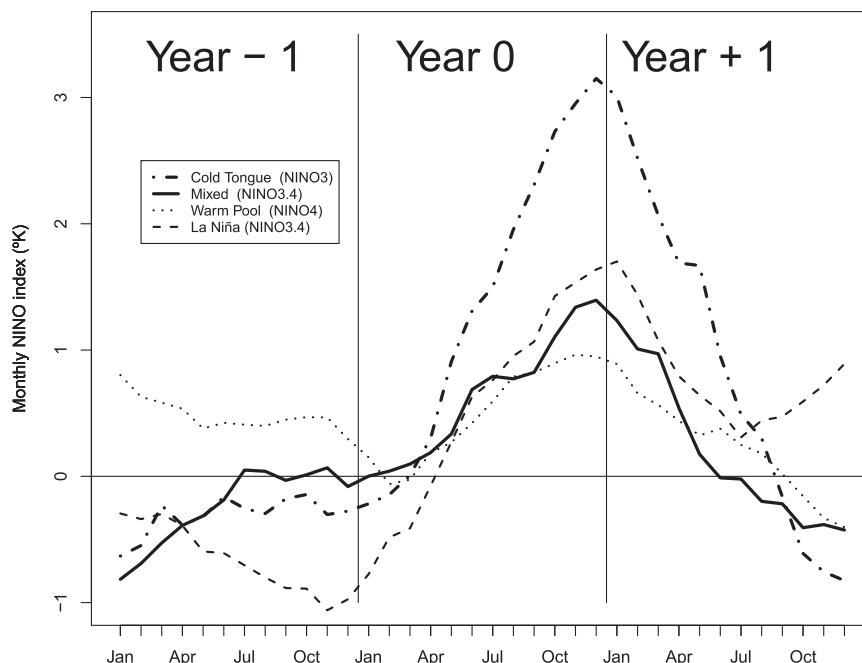
FIG. 3. Mean annual cycles of Niño indices for the three El Niño types and for La Niña events for 36 months starting January the year before the event until the December of the year after the event. The curve for La Niña events is inverted for comparison. Data are from the HadISST reanalysis, 1979–2011.
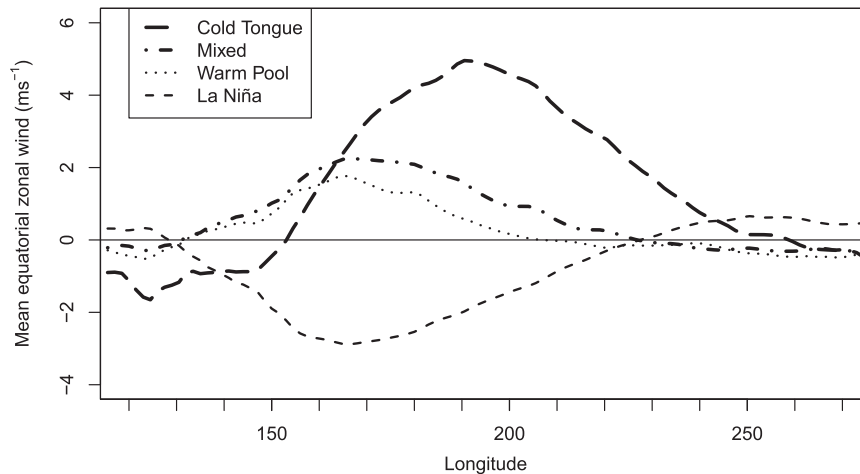
FIG. 4. Mean wind anomalies along the equator for the three El Niño types and for La Niña across the equatorial Pacific. Data are from the ERA-Interim reanalysis, 1979–2010, averaged from 5°S to 5°N. Positive (negative) values indicate westerly (easterly) anomalies.

Year 0, but there is little change from October to January. ME and CTE decay more rapidly than WPE. CTE tend to persist until later, staying above 1.0°C until June in Year +1 (as noted by other studies, e.g., Lengaigne and Vecchi 2009). By the end of Year +1 all El Niño types have negative indices; in ME Niño-3.4 becomes negative in June whereas this occurs later in CTE and WPE events. CTE indices reach the most negative values: the 1997/98 CTE and 1987/88 ME were both followed by La Niña events. La Niña Niño-3.4 (which is multiplied by −1 in Fig. 3) warms to a peak around 1.0°C in December of Year −1, a consequence of four of the five La Niña having been preceded by an El Niño. The mean La Niña Niño-3.4 cools during Year 0, falling below zero in May and reaching peak magnitude in January of Year +1. The Niño-3.4 anomalies then decay but remain negative throughout Year +1, reflecting the tendency of some La Niña events to redevelop the following year (as in 1998/99 and 2010/11).

b. Surface wind characteristics

The strength and direction of the trade winds are characteristic features of ENSO, comprising the surface component of the Walker circulation. In this section we describe how the surface winds respond to the shifts in convection zones linked to SST anomalies during El Niño and La Niña events.

The September–February mean surface wind anomalies for each El Niño event type and La Niña are shown in Fig. 2. La Niña events show a strengthening of the trade winds, particularly along the equator, while El Niño events show westerly wind anomalies (weaker equatorial trades) to varying degrees. All three El Niño types have mean westerly equatorial zonal winds in the western to

central Pacific, from 125° to 165°E for WPE, from 125° to 170°E for ME, and from around 157° to 195°E (165°W) for CTE. The equatorial westerly wind anomalies are located about 30° to the east for CTE compared to the other El Niño types (Fig. 4) and they are much stronger than the other types (more than twice the ME, which are in turn stronger than the WPE anomalies). The magnitude of the maximum equatorial zonal wind anomaly scales with the mean strength of the Niño anomalies for all El Niño types to very similar degrees [a factor of approximately 1.8–2.1 of $\Delta(\text{m s}^{-1})/\Delta(°C)$]. As the largest positive SST anomalies of the El Niño type moves eastward so too does the region of maximum westerly wind anomalies. The zonal extent of the westerly wind anomalies is also largest for CTE; although they both begin around 130°E, the ME anomalies extend much farther east than those of WPE. La Niña equatorial wind anomalies mirror most closely the response in ME events, as did their SST anomaly patterns.

The strongest westerly wind anomalies are located just south of the equator, although this region of maximum anomalies moves from north to south of the equator around November (McGregor et al. 2012). CTE events also show very strong anomalous meridional convergence of surface winds in the western and central Pacific toward this latitude of strongest westerly anomalies south of the equator. This convergence is evident between 10°N and 20°S, latitudes that coincide with the mean positions of the ITCZ and SPCZ respectively. This surface convergence is also present but much weaker for the other El Niño types (mean meridional wind magnitudes for ME and WPE between 10°N and 20°S and 160° and 200°E are 55% and 40%, respectively, of the CTE values). There is somewhat weaker divergence from the
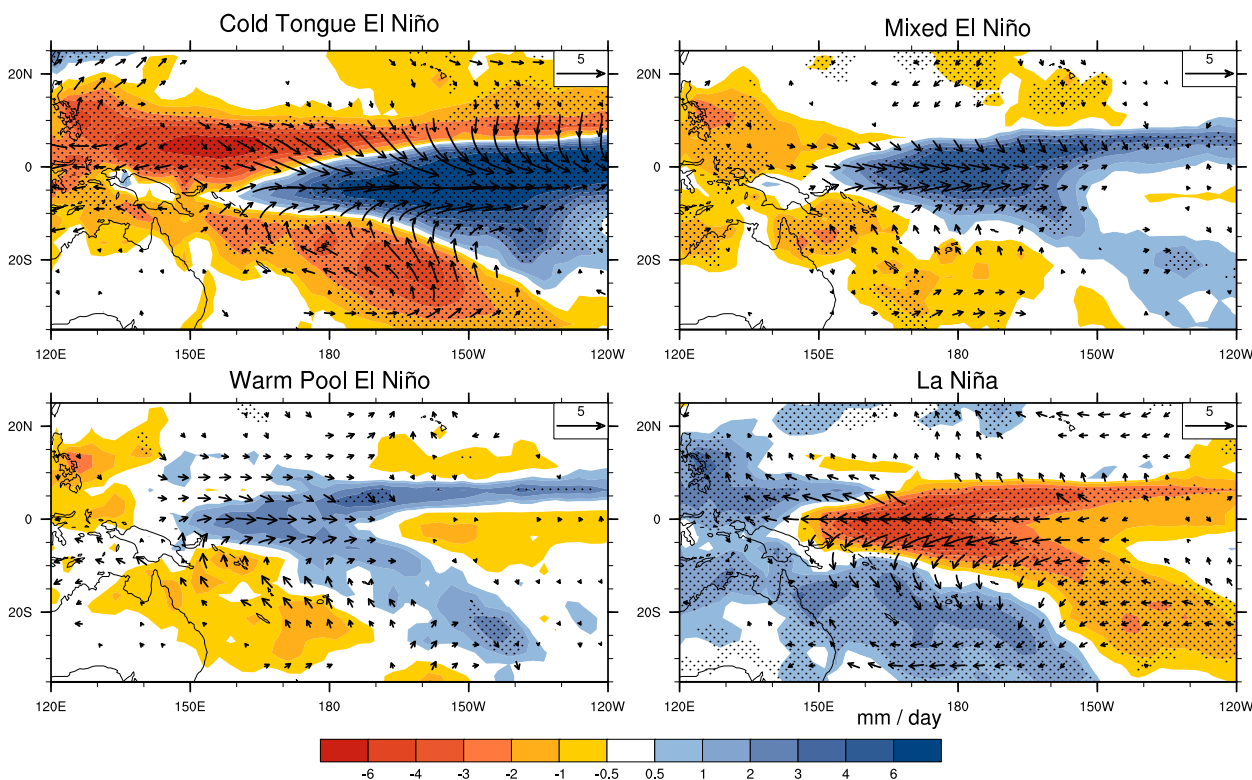
FIG. 5. Mean November–April rainfall anomalies (mm day^{-1}) for the three El Niño types and for La Niña events. Arrows show the corresponding surface wind anomalies for September–February, with the reference arrow denoting 5 m s^{-1}. Winds are only shown where wind anomaly exceeds 0.5 m s^{-1}. Stippling denotes where the rainfall anomalies are statistically significantly different from zero at the 90% confidence level. Rainfall data are from the GPCP analysis and wind data are from the ERA-Interim reanalysis, 1979–2010.

equator for La Niña (around 80% of CTE). The surface winds respond to the SST anomalies that accompany each event. The main zones of convection move in response to changes in SST patterns, with surface winds converging into these convective zones.

c. *Large-scale precipitation characteristics*

The large-scale precipitation response to the different types of El Niño events and La Niña is shown in Fig. 5. The response in rainfall in November–April shows a very clear relationship to the SST and wind changes. The strongest positive anomalies are seen for CTE, peaking in the eastern equatorial Pacific. The positive mean ME rainfall anomalies are somewhat weaker than the CTE anomalies and are situated farther west, centered on the date line. They are also closely mirrored by the mean La Niña pattern. Positive WPE rainfall anomalies are weakest and generally farthest west and are mostly not statistically significant. In each case the SST anomalies and wind responses are accompanied by changes in the strength and position of the main convergence zones, altering rainfall patterns.

During CTE, large, extensive, statistically significant rainfall changes occur: increases along the equator to the

east of the Solomon Islands and decreases throughout the southwest or south central Pacific, and across most of the basin north of about 5°N. This results from the SPCZ moving far north of its usual November–April position and the ITCZ moving south, as shown by other studies (Vincent et al. 2011, Cai et al. 2012). These studies also found a similar "zonal" SPCZ behavior in the 1991/92 El Niño, although to a lesser extent, probably due to the weaker SST anomalies compared to 1982/83 and 1997/98 and the shift of the strongest SST anomalies to the central Pacific. During the two CTE November–April periods, the ITCZ and SPCZ have essentially merged to form a single convergence band straddling about 7°S, widening farther to the east (Fig. 6, and also in the mean north–south rainfall profile along 200°E; Fig. 7b). There is only one rainfall maximum at 7°S; no local maxima are seen at the usual positions of the ITCZ and SPCZ (around 7°N and 12°S respectively). The maximum of 12.8 mm day^{-1} is close to the sum of the two ITCZ and SPCZ maxima of the mean rainfall for all November–April seasons (7.3 and 6.4 mm day^{-1}). The longitude of the maximum equatorial rainfall has also moved eastward from around 150°E to around 215°E and has increased from 9.3 to 11.2 mm day^{-1} (Fig. 7a).
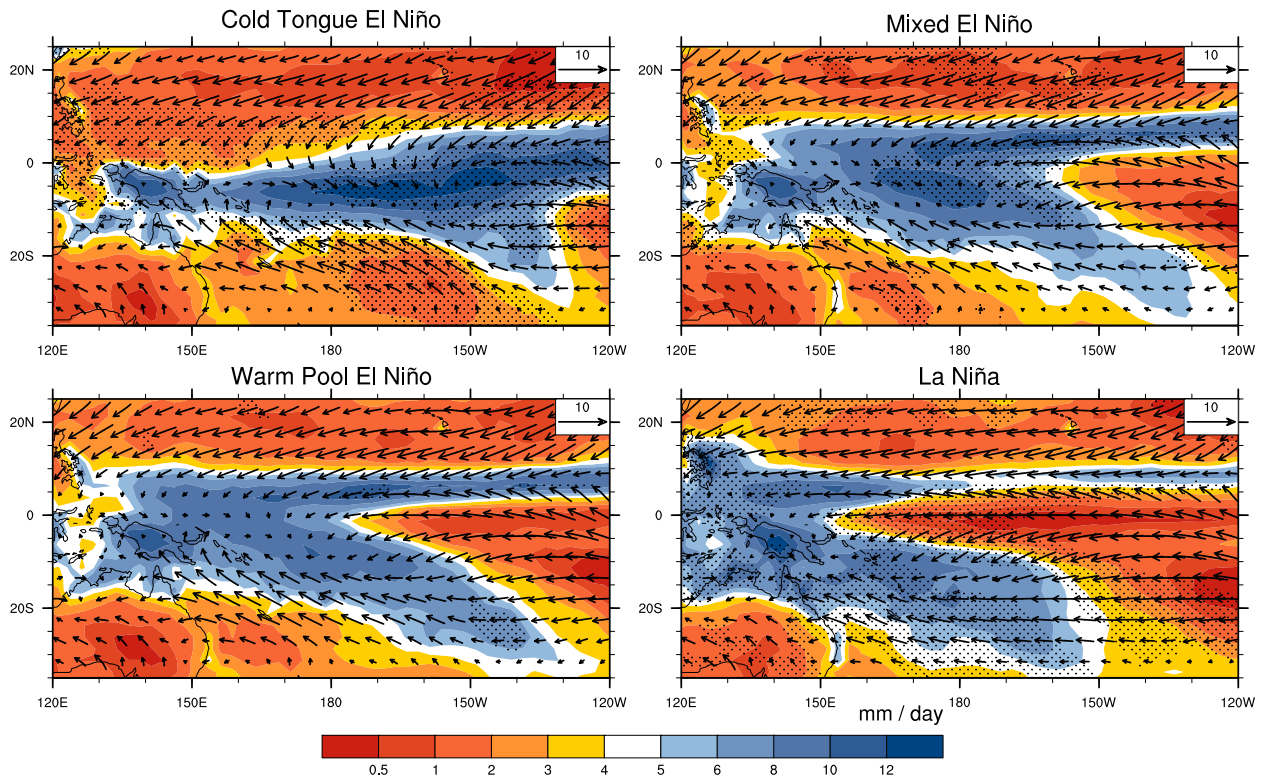
FIG. 6. Mean November–April rainfall totals for the three El Niño types and for La Niña events. Arrows show the corresponding mean surface winds for September–February, with the reference arrow indicating $10\,\mathrm{m\,s^{-1}}$. Rainfall data are from the GPCP analysis and wind data are from the ERA-Interim reanalysis, 1979–2010.

The SPCZ and ITCZ do not merge in the other El Niño types (Figs. 6 and 7b). For ME we see increased rainfall close to the SPCZ and ITCZ mean positions, although both have moved relative to mean conditions (Figs. 5 and 6): north and south, respectively. The largest decrease in rainfall in the Southern Hemisphere occurs in the southwest Pacific as the SPCZ moves northeastward. The largest decrease in the Northern Hemisphere occurs in the far northwest tropical Pacific and over parts of the Marshall Islands and to their east as the ITCZ moves southward. Along the equator the rainfall maximum has moved eastward compared to neutral conditions to near 175°E and increased from 9.2 to $10.7\,\mathrm{mm\,day^{-1}}$ (Fig. 7a). Along the 200°E transect the ITCZ maximum has moved slightly southward (Fig. 7b; compare with neutral years), while the SPCZ maximum has strengthened and moved northward, with rainfall decreasing on its southern edge: equatorial rainfall has intensified from 0.9 to $4.6\,\mathrm{mm\,day^{-1}}$ (Fig. 7b). The area of statistically significant rainfall changes is smaller than for CTE events, being generally confined to the ITCZ and SPCZ regions and along the equator either side of the date line. Some changes in the southwest, northwest, and northern Pacific are also statistically significant.

As expected from the weaker SST and wind anomalies associated with WPE, the rainfall anomalies are also weaker and smaller in extent, and the area of statistical significance is further reduced (Fig. 5). The total rainfall pattern (Fig. 6) is similar to that for ME, but most of the anomalies are not significant. The anomalies show rainfall increasing along the ITCZ and SPCZ, but the SPCZ does not move as far to the northeast as in ME years. Along the equator the rainfall maximum only increases in strength by about $0.5\,\mathrm{mm\,day^{-1}}$ and moves about 10° to the east. Along 200°E rainfall shows a small increase from neutral conditions on the northern edge of the SPCZ and a slight decrease on its southern edge, showing a small shift northward (Fig. 7b). Drier conditions occur east of about 170°W, contrasting with the CTE years. There is a suggestion of increased rainfall in WPE years in the western Pacific around 10°N extending through parts of the Federated States of Micronesia to near Palau (see Fig. 5), although the anomalies are not significant. This appears to be driven by positive SST anomalies in this region, which is not seen for the other El Niño types.

La Niña years show large areas of statistically significant rainfall changes, largely the opposite of the ME
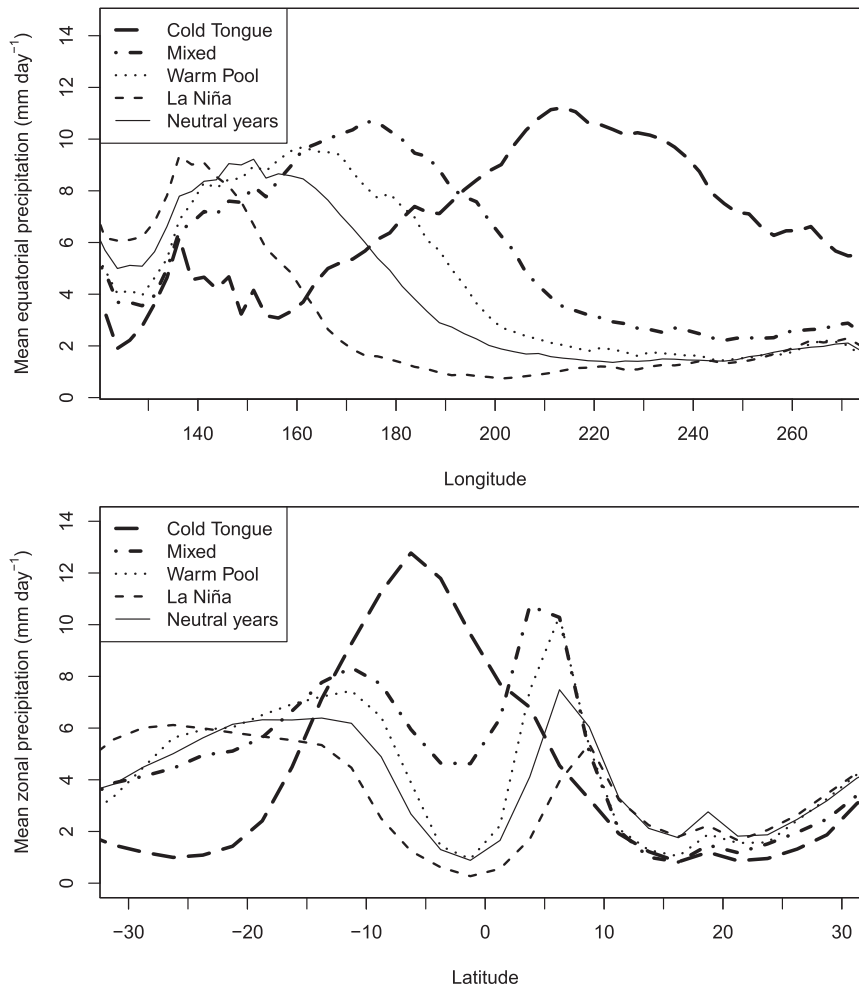
FIG. 7. Mean rainfall totals along the equator for the three El Niño types, for La Niña and for ENSO neutral years: (a) along the equator (averaged from 5°S to 5°N) and (b) north–south along 200°E (averaged from 195° to 205°E). Data are from the GPCP analysis, 1979–2011.

pattern. Some differences occur; for example, the near-equatorial anomalies extend farther east and west. The La Niña rainfall anomalies also show a region of drier conditions extending into the northwest Pacific that mirror the wetter region in the WPE pattern there, although neither of the anomalies in this region is statistically significant at 90%. Given the large area of significant changes evident, the La Niña pattern appears to be more coherent and robust than the WPE and ME patterns. Overall, countries that experienced suppressed rainfall in ME also received enhanced rainfall during La Niña.

As with SST and surface winds, CTE and La Niña events show the biggest and most significant rainfall anomalies over much of the equatorial Pacific. While the ME rainfall anomalies are smaller than those in CTE events, most of the anomalies greater than 1 mm day^{-1} are statistically significantly different from zero. Figure 8

(left column) shows the differences between the CTE and ME composite SST and rainfall patterns, to illustrate how different they are. In WPE the rainfall response is broadly similar to ME but weaker and areas of significant anomalies are very small, reflecting the weaker SST and wind anomalies. To determine if the WPE rainfall response can actually be differentiated from the ME response, the difference between their rainfall patterns is shown in Fig. 8. There are large and significant differences between their SST patterns as expected, with ME warmer in the Niño-3.4 region and WPE warmer to the west. The rainfall patterns show the expected differences, but most differences between the two types of event are not statistically significant. Only over a few countries in Fig. 1 can the rainfall anomalies between ME and WPE be said to be significantly different (Kiribati, the northern Cook Islands, Palau, and western Federated States of Micronesia). There are
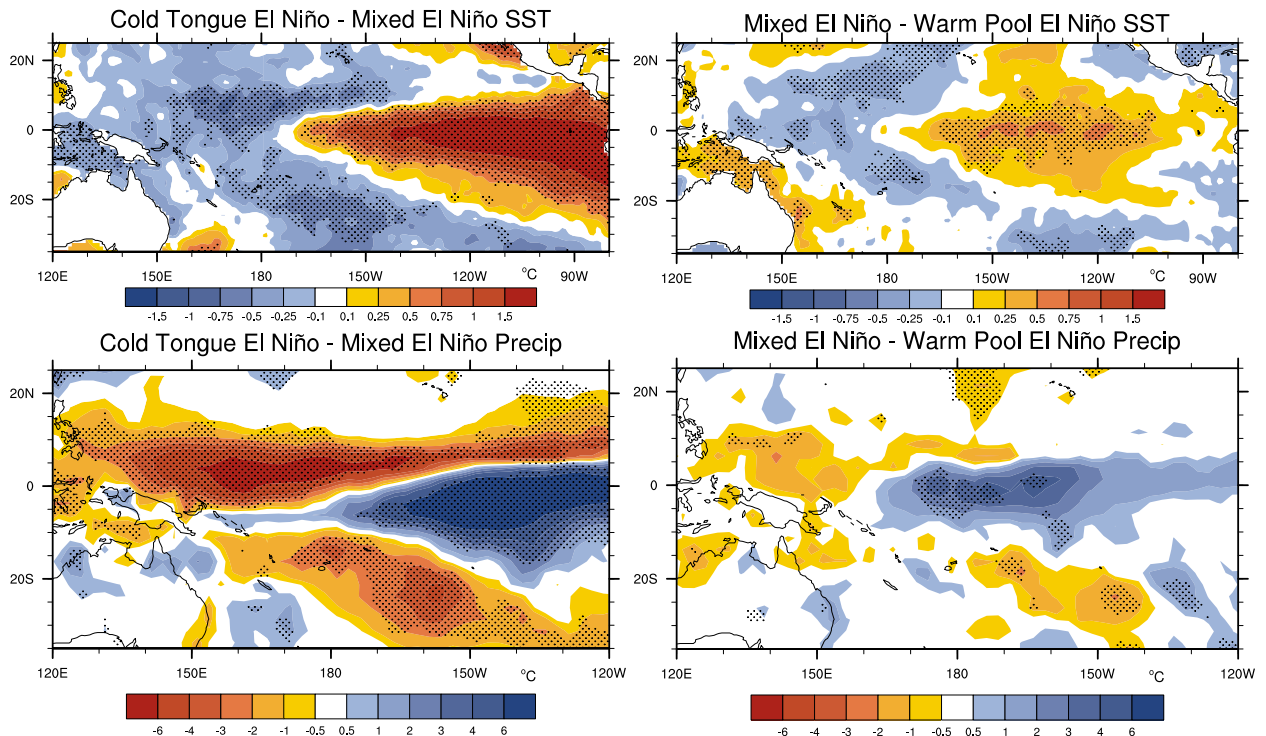
FIG. 8. Difference in (top) SST and (bottom) precipitation between (left) mean cold tongue El Niño and mixed El Niño and (right) mean mixed El Niño and west Pacific El Niño events. Stippling denotes where the anomalies are statistically significantly different from zero at the 90% confidence level. Data are from the HadISST and GPCP analysis, 1979–2011.

other regions where the rainfall differs, such as over parts of French Polynesia. Thus, while CTE and ME El Niño events have significant rainfall anomalies over many Pacific islands, WPE does not; over most countries its rainfall response is not significantly different from ME events. This will be explored further in section 5, but WPE appears to be a variant on the ME rather than a separate El Niño type of its own. This is partly as expected from the definitions; WPE anomalies are confined to the western Pacific, while the other El Niño types have SST anomalies over much larger areas.

4. El Niño and La Niña rainfall impacts at specific stations

The distinct rainfall anomaly patterns for the El Niño types suggest that countries in the equatorial, northwest, and southwest Pacific in particular should experience quite different impacts for CTE when compared to the other El Niño types. In this section we examine rainfall at specific locations in the Pacific island countries in these regions. A longer period (1950–2011) is used as rainfall data from the stations is available further back in time than the GPCP rainfall dataset. However, we only categorize years into El Niño, neutral, and La Niña (not

into different El Niño types) and we highlight the CTE years 1982/83 and 1997/98.

Mean November–April rainfall and interannual standard deviations were calculated at each station from 1950–2011 (Table 1). Many stations show very large interannual variability in wet season rainfall relative to the mean. For example, Tarawa in Kiribati has a mean November–April rainfall of 1186 mm and a standard deviation of 727 mm. Its November–April total rainfall was 2440 mm in 1986/87 but only 140 mm in 1988/89.

We now illustrate some of the variations in rainfall response to ENSO across the region. More detailed analysis at each country will follow, but first we show time series of November–April rainfall anomalies from 1950–2011 and the ENSO phase each year for several stations (Fig. 9). We limit this to six stations across the three climate regions that displayed either quite different impacts between CTE and the other El Niño types in the analysis above, or where the ENSO impact was unclear (NWP, SWP, and EP: see Fig. 1 and Table 1). These plots are color-coded with the phase of ENSO [all El Niño (red), neutral (black), and La Niña (blue)]. Interannual variability in November–April rainfall in most of these stations is closely related to ENSO, Funafuti (Tuvalu) being the exception. Nauru and Tarawa
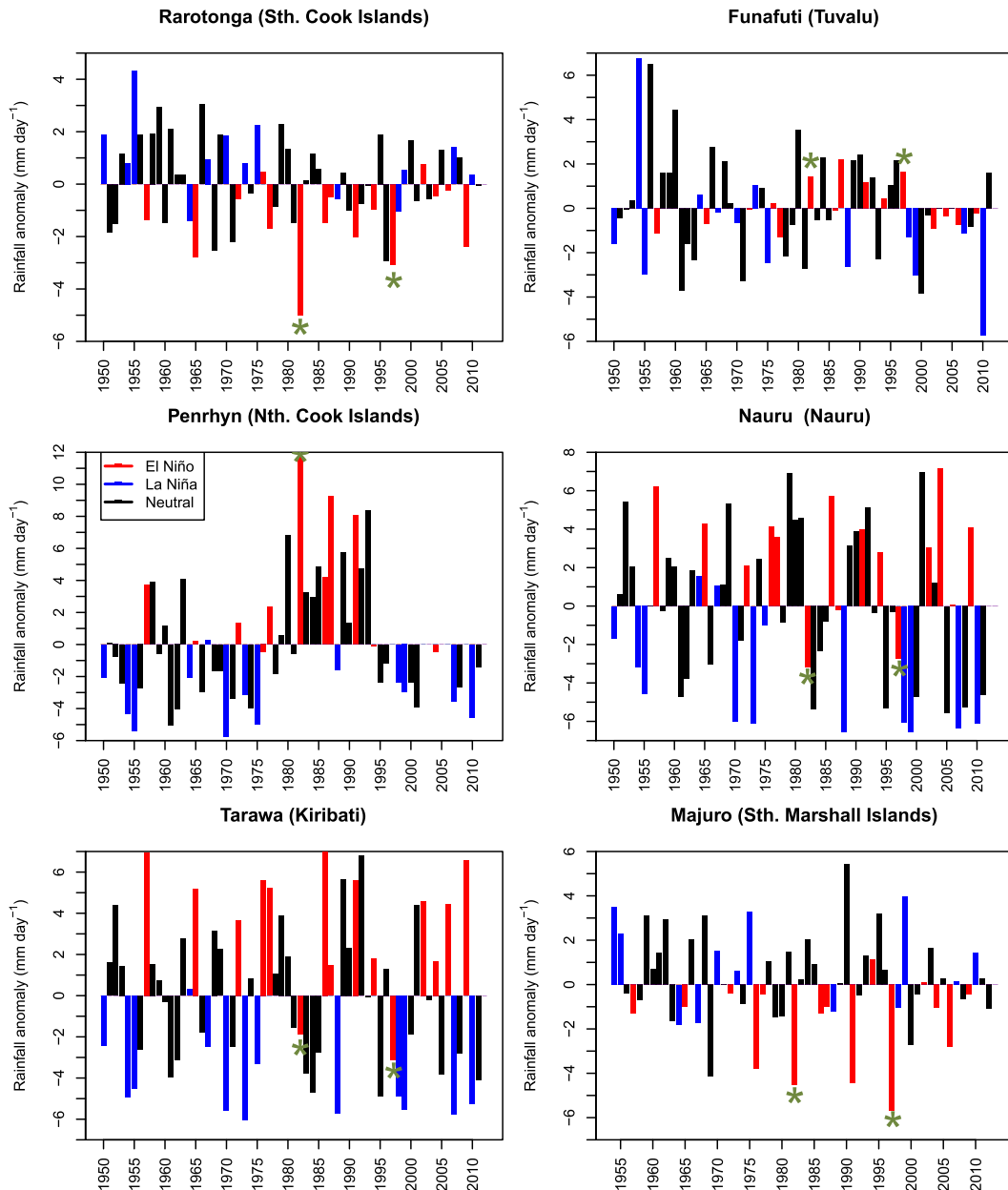
FIG. 9. Mean November–April rainfall from stations in the Pacific for each year 1950–2009. The year is that of November. Red bars denote El Niño years, blue bars La Niña years, and black bars neutral years. 1982 and 1997 are marked by asterisks. Note that insufficient data are available for Penrhyn in 1997 so no asterisk is shown.

(Kiribati) have very clear impacts (wet El Niño and dry La Niña). The coherent El Niño SST warming and La Niña cooling seen in Fig. 2 in the region surrounding these western equatorial Pacific countries leads to rainfall being directly enhanced or suppressed, respectively (Fig. 5), hence the clear relationship with ENSO phase. The exceptions in these countries are the two CTE years 1982/83 and 1997/98, which were both drier than normal rather than the usual El Niño

enhanced rainfall. These two years are marked with an asterisk in Fig. 9 as they show atypical El Niño rainfall behavior in these and other countries.

Majuro (Marshall Islands, in the NWP region) has a mixed response to ENSO phases, but tends to have wet La Niña and dry El Niño years. The CTE years 1982/83 and 1997/98 were the two driest years in this record. The two Cook Island stations (in the SWP region), Rarotonga (in the south) and Penrhyn (in the north),

show very clear ENSO signals but of opposite signs; the stations are approximately 1185 km apart. El Niños are generally dry in the south and wet in the north, with La Niña events having opposite signals. The two CTE years are also unusual: 1982/83 was the wettest year on record in Penrhyn and the driest in Rarotonga (where 1997/98 was also the second driest). This difference explains the lack of clear ENSO signal in Funafuti (Tuvalu). This island is near this transition from wet to dry El Niño impacts (see Fig. 5) so shows no consistent signal. However, it does have more of a tendency to experience dry conditions during La Niña events.

An atypical November–April rainfall signal in 1982/83 and 1997/98 CTE events is also apparent elsewhere: Banaba (not shown) in Kiribati (near Tarawa) had drier than average November–April periods in these two years when wetter than normal conditions usually occur in El Niño years. Other sites experienced rainfall extremes in those two years: Nanumea (not shown) in Funafuti (400 km northwest of Funafuti), which experiences wetter than average El Niño and drier La Niña wet seasons, had its two wettest November–April periods on record; Pohnpei, Yap, and Chuuk in the FSM and Koror in Palau, which are usually drier in El Niño and wetter in La Niña events than average, all had their two driest November–April periods on record.

The atypical or extreme rainfall experienced in these CTE years in many countries is consistent with the extreme shift and change in intensity in the SPCZ and ITCZ seen in Fig. 6, as noted by other studies (Vincent et al. 2011; Cai et al. 2012). It is clear that large-scale mechanisms in CTE years brought about quite different impacts from those in other El Niño events. The rainfall changes in the EP region countries were completely different from those for other El Niño types. It would appear that the two CTE years were unique in this respect—all other El Niño years brought increased rainfall at Tarawa, for example, and all La Niña years brought below average rainfall. These rainfall anomalies of opposite sign in these countries for CTE would be expected to reduce linear correlations between the Niño and rainfall (e.g., the correlation between Niño-3.4 and November–April rainfall in Tarawa increases from 0.71 to 0.85 when 1982/83 and 1997/98 are excluded).

The time series in Fig. 9 also indicate no clear interdecadal variation in the rainfall response to ENSO in these countries except at Penrhyn. The Pacific decadal oscillation (PDO) and the equivalent (in terms of impact in the tropical Pacific) interdecadal Pacific oscillation (Folland et al. 2002) have been shown to vary the influence of ENSO on rainfall in some countries in the Pacific rim, such as Australia (Power et al. 1999). In some Pacific countries its influence has been shown to be minimal (e.g. Cambers et al. 2011). We have calculated mean November–April rainfall anomalies at the 19 stations listed in Table 1 for the three different phases of the PDO since 1950 (1950–76, 1977–99, and 2000–11) for all El Niño types and La Niña, and found no clear regional PDO signal in the rainfall anomalies at the stations associated with ENSO.

5. Impacts of El Niño types and La Niña events in Pacific island countries

Having shown that clear ENSO impacts are evident in many countries in the Pacific, and that CTE years have quite different impacts in some countries from the other El Niño types, we now focus on impacts in all 15 countries included in the study. In this section we examine in more detail the differences and consistencies in temperature and rainfall responses across El Niño types and also across the years that fall into each El Niño category. We first examine country-scale impacts and then look at individual stations.

a. Country-scale ENSO impacts

This section investigates the ENSO-related changes in SST and rainfall over each of the 15 countries listed in Table 1. For each country a region is defined, corresponding to the Exclusive Economic Zone (EEZ) of the country. Several of the larger countries are subdivided: the Cook Islands and Marshall Islands into north and south regions, and the Federated States of Micronesia into east and west regions. Kiribati is divided into three regions: from west to east, Kiribati (the Gilbert Islands), the Phoenix Islands, and the Line Group. The regions are listed in Table 1. As we use large-scale rainfall analysis fields, the period considered here is 1979–2011.

To examine the consistency across the various El Niño types, we calculated the mean SST and rainfall anomalies for each El Niño type and La Niña over each country, being the average over each region from the maps in Figs. 2 and 5.

SST anomalies (Fig. 10a) generally show cooling during El Niño and warming for La Niña events in the countries in the far west, southwest, and northwest Pacific, with the opposite changes close to the equator east of about 170°E. CTE SST anomalies tend to be strongest over most countries except those in the Niño-4 or Niño-3.4 regions: Tuvalu, the northern Cook Islands, Nauru, Kiribati, and the Phoenix Islands. Major differences in the anomalies between El Niño types are seen in some countries. The Marshall Islands show opposite SST anomalies in CTE compared with other El Niño types. PNG, Solomon Islands, Niue, and the southern Cook Islands have cool SSTs for CTE, but anomalies close to zero for ME and
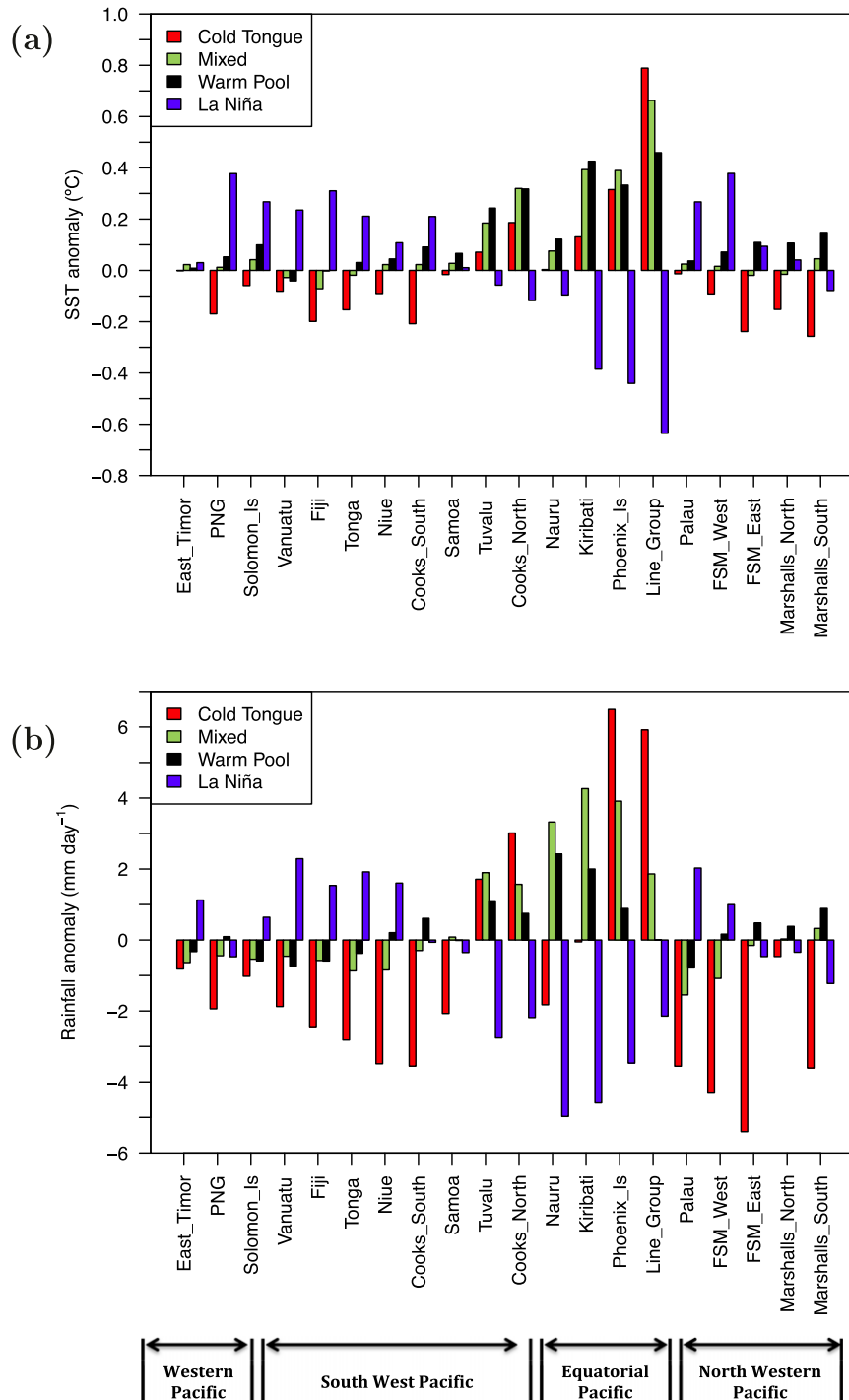
FIG. 10. Spatially averaged mean anomalies of (a) SST (for September–February) and (b) rainfall (for November–April) for the 3 El Niño types and La Niña events over the EEZ of 15 countries (with several subregions) in the Pacific and East Timor. Stations are ordered by geographical proximity into regions given below the figure. SST data are from HadISST and rainfall data are from GPCP for 1979–2011.

TABLE 3. Summary of the impacts of El Niño types and La Niña on November–April rainfall in each country and region, showing whether there is a clear wet or dry signal. Bold type indicates the anomalies at stations are statistically significant at the 90% level. The linear correlation coefficient between the November–April rainfall anomalies at stations and each region from the large-scale reanalysis from 1979–2011 is also shown (r GPCP/station).

Country	Region/station	r GPCP/ station	CTE	ME	WPE	La Niña
East Timor	Dili	0.32	Wet			
PNG	Kavieng	0.53	Wet			Dry
Solomon Islands	Honiara	0.73	**Dry**	**Dry**	Dry	**Wet**
Vanuatu	Port Vila	0.74	Dry	Dry		Wet
Fiji	Nadi	0.81	Dry	**Dry**		**Wet**
Tonga	Nuku-alofa	0.84	Dry	Dry	Dry	Wet
Niue	Hanan	0.77	**Dry**	**Dry**		**Wet**
Cook Islands	North/Penrhyn	0.76	Wet	Wet		**Dry**
	South/Rarotonga	0.54	**Dry**	**Dry**	**Dry**	**Wet**
Samoa	Apia	0.66	Dry	Dry	Dry	Wet
Tuvalu	Funafuti	0.68	Wet			Dry
Nauru	Nauru	0.95	Dry	**Wet**	**Wet**	**Dry**
Kiribati	Tarawa	0.96	Dry	**Wet**	**Wet**	**Dry**
	Phoenix Islands (no station)		**Wet**	**Wet**		**Dry**
	Line Islands/Kiritmati	0.76	**Wet**	Wet		Dry
Palau	Koror	0.80	**Dry**	**Dry**	Dry	Wet
Federated States of Micronesia	West/Yap	0.78	**Dry**	**Dry**		**Wet**
	East/Pohnpei	0.64	**Dry**			**Wet**
Marshall Islands	North/Kwajalein	0.57	**Dry**			Wet
	South/Majuro	0.50	**Dry**	**Dry**		Wet

WPE; and Tuvalu and Nauru have zero anomalies for CTE but positive anomalies for ME and WPE.

For rainfall, different responses among the El Niño types are even more apparent (Fig. 10b). The countries that normally sit under the influence of the SPCZ, from the Solomon Islands to Samoa, have quite strong rainfall reductions in November–April in CTE years, indicating the large changes when the SPCZ becomes zonal and moves far to the north. Only weak rainfall anomalies are seen in these countries in other El Niño years. The magnitude of the positive La Niña anomalies tend to lie somewhere in between. The northern Cook Islands experience the opposite impacts from those in the southern part of country (cf. Fig. 9). Very different responses are also seen for La Niña years: dry conditions in the north but little mean impact in the south. In Nauru and Kiribati much wetter than normal conditions are seen in ME and also, but to a lesser extent, in WPE, whereas CTE are drier than normal due to the eastward shift of the SPCZ and ITCZ away from these countries. Extremely dry La Niña years are observed due to a northward displacement of the ITCZ and a southwest displacement of the SPCZ.

The southward shift of the ITCZ to the equator in CTE has a very strong impact in the northwest Pacific countries. All except the northern Marshall Islands are extremely dry in CTE years. Impacts on rainfall are much smaller in other El Niño years, except ME events are dry in Palau and western FSM; all anomalies are very weak for WPE. In the Marshall Islands and eastern FSM, both CTE and La Niña events tend to reduce rainfall. In Fig. 6 it can be seen that in La Niña years the ITCZ is less extensive and contracted to the south, with a consequent reduction in rainfall.

b. Local-scale ENSO impacts at individual stations

The previous section deals with large-scale responses over relatively large areas. Here we use data from individual observing stations (listed in Table 1) in order to reveal any local-scale effects.

We first compare the time series of November–April rainfall anomalies from stations from 1979 to 2011 with those from the country/region-scale analysis above using GPCP analysis. The linear correlation coefficients at the 19 stations/regions between the station and analysis datasets are given in Table 3, and their mean value is 0.70. The only region with a correlation significantly lower than the average is East Timor/Dili, where the complex topography of the country means Dili is not representative of the country as a whole. The ENSO impacts across the El Niño types and La Niña in most countries should then be broadly consistent across the two data sources; the results below will be considered in light of the differences.

We also compared mean rainfall anomalies from each region for each El Niño type and La Niña from the large-scale GPCP analysis (from Fig. 10b) to those at corresponding station in the same regions (Fig. 11). We find
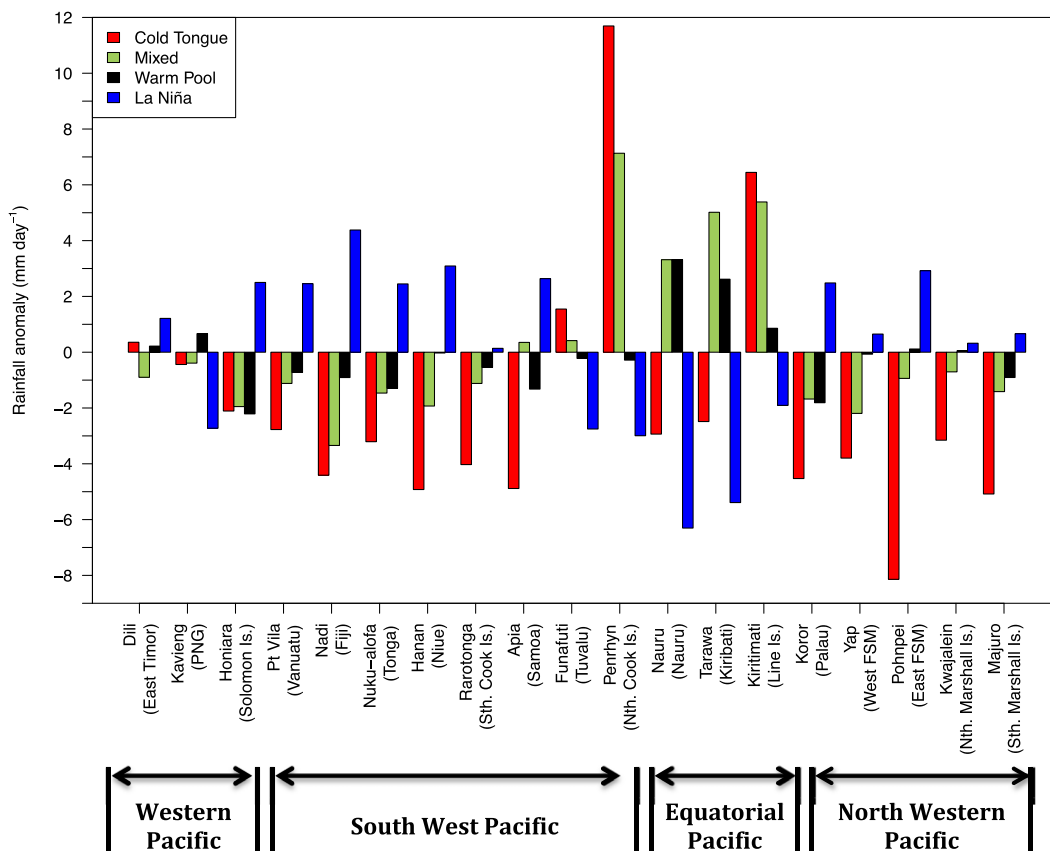
FIG. 11. Mean November–April rainfall anomalies from 1979–2011 at stations in each of the regions in Fig. 10 for the three El Niño types and for La Niña events.

the correlation coefficient between the two sets data is 0.83, showing that most of the ENSO variability at the individual stations in the November–April rainfall is captured through changes in large-scale rainfall patterns reflected in the analysis. Differences at the station level from the large scale reflect local-scale influences on rainfall. The PNG (Kavieng) impacts are quite different from the whole of PNG but no one station will necessarily reflect the impacts over such a large, geographically complex country. Other regions also have some disagreement between station data and the large-scale analysis, mostly in large regions that have in-country variations in ENSO impacts. This suggests that the station is not representative of the whole region used in the GPCP analysis results.

We now examine rainfall anomalies at each station for each individual El Niño and La Niña year. We extend the period to 1950–2011. This involves extending the classification of El Niño and La Niña events back to 1950, despite the lower quality of the SST data before 1979. Between 1950 and 1978, 1977/78 was found to be a WPE (as in KUG09), and two ME (1957/58 and 1965/66), two

CTE (1972/73 and 1976/77, as in KUG09), and eight La Niña events were found (1950/51, 1954/55, 1955/56, 1964/65, 1967/68, 1970/71, 1973/74, and 1975/76); this earlier period was dominated by La Niña events. The statistical significance of the anomalies is also assessed by a Student's t test; if the mean anomaly for each event type was significantly different from zero at the 90% level it is plotted as a solid shape (Fig. 12).

Overall, La Niña events show the largest number of statistically significant rainfall responses at the stations: nine of the 19 stations shown have statistically significant mean rainfall anomalies for La Niña. At some stations the sign of change is inconsistent across La Niña events, so the mean changes are not significant: this was the case at Dili, Kavieng, Port Vila, Funafuti, Kwajalein, and Majuro. At Nuku'alofa, Apia, Kiritimati, and Koror the lack of a statistically significant mean change is due to the small anomalies in most La Niña events. However, at some stations, Rarotonga and Yap in particular, small anomalies during La Niña events are very consistent in sign across events such that the mean anomalies are still statistically different from zero.
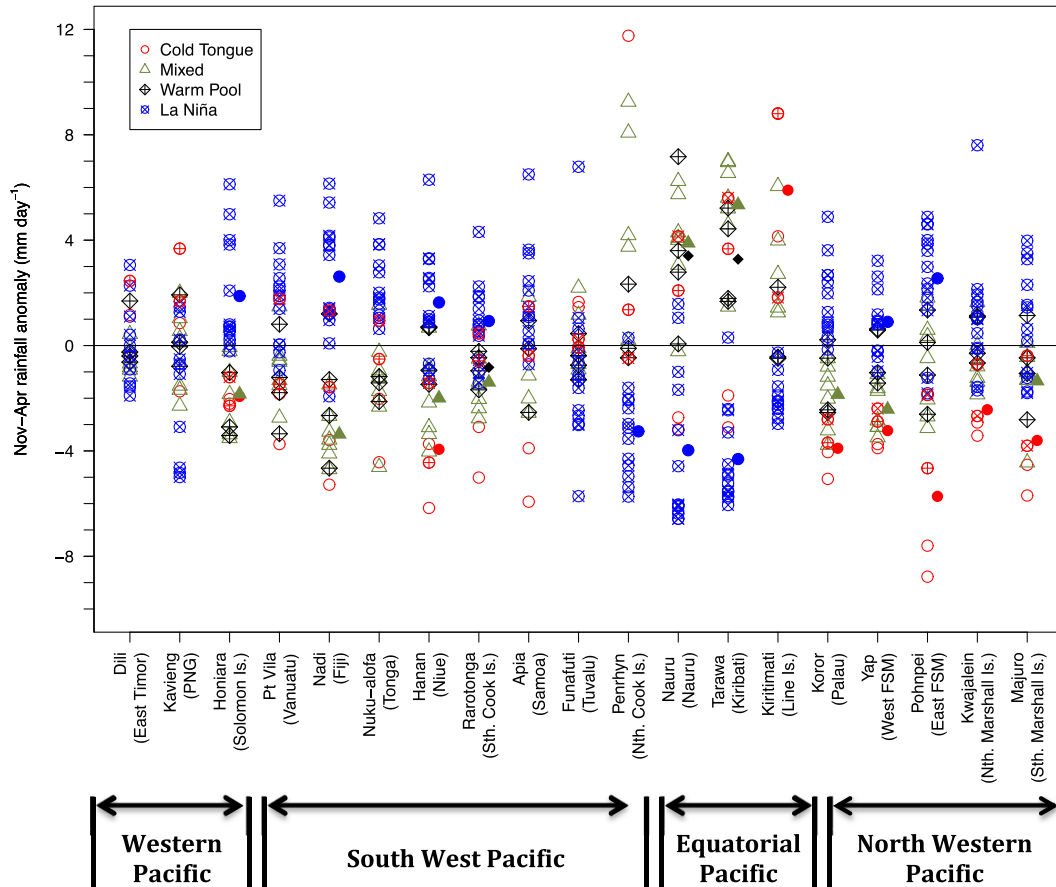
FIG. 12. November–April rainfall anomalies for each El Niño and La Niña event from 1950–2011, separated by event type. The mean anomaly for each event type is also plotted as solid shapes if the mean differs significantly from zero at the 90% level. The mean anomaly is not plotted if this criterion is not met.

Eight stations show significant rainfall anomalies during CTE, including all five in the tropical northwest Pacific region, and one in each of the other three regions. In all NWP stations all four CTE events had negative rainfall anomalies, but at each 1982/83 and 1997/98 were the two strongest; 1972/73 and 1976/77 had much weaker anomalies at some stations. At all other stations the November–April anomaly in 1976/77 was either very small or of the opposite sign to the other years. This is also the case for 1972/73 at all stations excluding those in the WP region and in Niue. Also evident is that in the countries where the zonal SPCZ events bring extreme or unusual impacts, both 1972/73 and 1976/77 brought very different rainfall impacts than 1982/83 and 1997/98. Penrhyn in the northern Cook Islands had missing data for the 1997/98 event but the anomaly in 1982/83 was more than 2000 mm (>3 standard deviations). However, the 1972/73 and 1976/77 anomalies were much weaker. This is also the case at Rarotonga in the southern Cook Islands and Funafuti in Tuvalu. In Nauru and Tarawa

1972/73 and 1976/77 actually had large but opposite rainfall anomalies to 1982/83 and 1987/88. The September–February Niño-3 anomalies in 1972/73 (1.8°C) and particularly 1976/77 (1.0°C) were weaker than in 1982/83 (2.6°) and 1997/98 (3.1°C), and it appears that their rainfall impacts were weaker or quite different as well. In the countries near the equator west of the date line the earlier two CTE events were not strong enough to reverse the usual wetter than normal El Niño pattern, and across the equatorial, western, and southwestern Pacific they generally brought much weaker rainfall impacts.

There are nine stations with significant mean anomalies across the ME. Even at stations where mean anomalies are not significant, there is generally a high degree of consistency in rainfall anomalies across the ME events. Only three stations show significant rainfall anomalies for WPE. This is because the anomalies for individual WPE years are usually lower than for the other categories, which is likely due in part to the weaker SST anomalies in these events, and anomalies of less

consistent sign. It may also be partly due to the earlier end to the WPE events (see Fig. 3). If the shorter December–February season is considered, the mean rainfall anomalies for WPE become significant at several stations in the southwest Pacific (Nadi, Port Vila, and Hanan). Only Nauru and Kiribati see relatively large rainfall positive anomalies. No stations have mean anomalies that are statistically significant across all El Niño types and La Niña.

If we compare to the results from the previous section at the country scale, there do appear to be robust rainfall responses in many countries and consistency across ENSO event types. The distributions of rainfall anomalies across the 19 stations for CTE are statistically significantly different from the ME and WPE rainfall anomalies (Student's t test p value < 0.05), but the ME and WPE anomalies are not significantly different (p value $= 0.85$). Only at Hanan (Niue), Penrhyn (northern Cook Islands), Kiritimati (Kiribati), and Yap (West FSM) are they significantly different (p value < 0.1). We also note again that 1972/73 and 1976/77 appear to be quite different CTE events from the others in terms of impacts. If only 1982/83 and 1997/98 are considered, four more stations reach significant mean anomalies for CTE years: Nadi, Funafuti, Nauru, and Tarawa. It appears that the impacts across the WPE, ME, and two earlier CTE events are relatively similar, while the two extreme CTE events were associated with quite different impacts to other events in many countries.

The impacts of the El Niño types and La Niña on November–April mean rainfall in the countries and regions are summarized in Table 3. There is a little disagreement between station data and the large-scale analysis, generally when a signal appears in the former but not in the latter. This suggests that the station is not representative of the whole region used in the GPCP analysis results. This is more likely to be the case in large regions that have in-country variations in ENSO impacts, such as Solomon Islands. In the southern Marshall Islands a dry signal in La Niña years is seen in the large-scale regions but the station (Majuro) shows a tendency toward wet conditions; the station lies close to the northern edge of the region and there is a sharp gradient in the sign of the signal.

In summary, SWP countries tend to have dry El Niño events: CTE events are the driest as the SPCZ moves far to the north, while WPE and ME events have smaller anomalies with smaller SPCZ shifts. La Niña years tend to be wet as the SPCZ shifts southwest. EP countries tend to have very wet El Niño years as the SPCZ and ITCZ shift equatorward, and very dry La Niña years (ITCZ and SPCZ move poleward). CTE are wettest for countries east of the date line but drier than normal to

the west where the convergence zones move away to the east. NWP countries generally have dry El Niño and wet La Niña years, with CTE being the most extreme as the ITCZ shifts away toward the equator. However, in the easternmost parts of those countries ME and WPE anomalies are weak, while La Niña can sometimes also be dry due to the a weakening and southward contraction of the northern edge of the ITCZ. In WP countries anomalies are much less consistent.

6. Discussion and conclusions

This study has examined the SST, wind, and rainfall changes that occur in the Pacific during El Niño and La Niña events and particularly how they impact island countries in this region. El Niño events were divided into three categories, the criterion being the location of the largest SST anomalies in the equatorial tropical Pacific.

The three El Niño types defined were warm pool El Niño (WPE) when the largest September–February SST anomalies occur in the western Pacific (Niño-4 region); mixed El Niño (ME) when they occur in the central-western Pacific (Niño-3.4 region); and cold tongue El Niño (CTE) when they are found farthest to the east (Niño-3 region). The large-scale SST, wind, and rainfall patterns were examined for each category and also for La Niña events. SST and rainfall impacts over Pacific island countries were calculated and rainfall responses found at individual stations in these countries.

It is found that CTE have the largest SST anomalies and the largest changes in surface winds, leading to the largest shifts in rainfall patterns in the main convergence zones. In the two CTE events since 1979, when high-quality satellite observations became available, the SPCZ and ITCZ moved equatorward and merged. Rainfall shifted east of the normal high rainfall zone over the west Pacific warm pool and was concentrated close to the equator. In the 15 countries examined, 11 of 19 stations showed consistent, statistically significant rainfall changes for these two events.

ME events had weaker SST anomalies than CTE, with the wind and rainfall responses being weaker as a consequence, as well as being located farther west. And for WPE the SST, wind, and rainfall responses are all weaker and farther west still. At the Pacific island country scale and at individual stations, the WPE have the least consistency and weakest rainfall impacts. The rainfall response was most consistent between individual La Niña and ME events.

The different large-scale atmospheric responses to the CTE, ME, and WPE events and the varying impacts in Pacific island countries support the classification based on the position of the largest SST anomalies. There is no

doubt CTE events are associated with the greatest rainfall impacts in most countries in the Pacific, although this is not always the case in the far western Pacific or over Australia (Wang and Hendon 2007). In some equatorial Pacific countries the CTE brings about the opposite rainfall changes to the other El Niño events. This has been found to be because the SST and wind changes in CTE years move the ITCZ and SPCZ equatorward and eastward, thus taking rainfall away from these countries.

In other El Niño events the rainfall in these convergence zones over these countries is enhanced by the local positive SST anomalies and enhanced wind convergence. In northwest and southwest Pacific countries, which sit under or near the edge of the SPCZ and ITCZ, CTE events have rainfall changes of generally the same sign as other events (mostly below average), but the anomalies are greater. In these countries we see that the large-scale changes in the SPCZ and ITCZ during CTE are large enough to shift rainfall away from the countries, whereas in ME and WPE years the shifts are not always large enough to consistently reduce rainfall: the countries still receive rainfall from these features as they have not moved far enough to completely remove their effect, although changes in rainfall still occur in many events.

These differences in rainfall changes are particularly important for countries in the Pacific for a number of reasons. First, in terms of seasonal ENSO prediction and its impacts on these countries it is clear that the detailed structure of the SST anomalies is important; it is not sufficient to predict the phase of ENSO or monitor ENSO using only one of the Niño indices. Many climate models suffer from SST biases, particularly in the extent of equatorial SST anomalies, with implications for the predicted impacts (Irving et al. 2011). Second, if CTE events do become more common in the twenty-first century (Cai et al. 2012), the frequency of unusual impacts may also increase, thus potentially changing the rainfall variability in some countries and affecting their ability to adapt.

The 1982/83 and 1997/98 CTE events were associated with atypical rainfall anomalies compared with other events. The two other CTE events (1972/73 and 1976/77) have weaker impacts on rainfall in most countries in the Pacific, and both earlier events had weaker SST anomalies. 1976/77 in particular is much more characteristic of other El Niño types in terms of the magnitude of the SST anomalies and the rainfall response. Our results also show that there are definite differences between the ME and WPE events: ME rainfall anomalies shift farther to the east than during WPE, and ME are accompanied by larger equatorward shifts of the SPCZ and ITCZ and enhancement of rainfall within them. However, while there are significant differences between ME and WPE rainfall anomalies over some countries, including some that we have not investigated (such as French Polynesia) and in regions where no countries exist, there is little to distinguish between rainfall impacts in ME and WPE events over many other countries. And indeed, the two weak CTE events show relatively similar impacts to WPE and ME events.

The atypical behavior of the two extreme events poses the question of whether the large magnitude of the SST changes is as relevant as the shape of the SST pattern or position of the largest anomalies. Some recent work has begun to address this question (Chung et al. 2014), but more investigation is planned using simulations of the historical climate record performed with coupled climate models and forced experiments with atmospheric general circulation models.

Previous studies, such as that of Takahashi et al. (2011), conclude that all El Niño events, both warm pool/central Pacific/Modoki and cold tongue/canonical, are part of the same category of El Niño, distinct from the extraordinary events of 1982/83 and 1997/98. We find differences in the rainfall responses depending on where the strongest SST anomalies occur, but the relative similarity of country-scale rainfall impacts during weak CTE events and the ME and WPE events seems to confirm the finding of Takahashi et al. (2011) that all events other than the two extreme El Niño events are "part of the same non-linear phenomenon." El Niño events are still different, as is the exact response of the climate in the Pacific to each, so this clarification should be regarded in the context of the very important impact ENSO has on rainfall in all countries in the Pacific region and the effects this has on the lives of its inhabitants.

APPENDIX

El Niño Classification Method and Comparison with Kug et al. (2009)

The basis of the classification of El Niño years is that used by Kug et al. (2009, hereafter KUG09). That study proposed a classification of El Niño events based on the September-to-February Niño-3 and Niño-4 indices. El Niño years were defined as those when either Niño-4 or Niño-3 exceeded their standard deviation, and events were classified as warm pool El Niño (WPE) if Niño-4 was largest, and cold tongue El Niño (CTE) when Niño-3 was largest. They also proposed a mixed El Niño (ME) with "features between the CT and WP El Niño events," defined as those for which "their maximum SST anomalies are located between 120° and 150°W." KUG09 used the improved Extended Reconstructed Sea Surface Temperature version 2 (ERSST) data (Smith and Reynolds 2004) from 1970 to 2005. In their study "Anomalies... are detrended after removing the monthly-mean climatology."

Our classification method is the same as that of KUG09 for the CTE and WPE events, using September–February Niño-3 and Niño-4 anomalies. However, there are a number of minor differences between the two methods. These include the following:

1) We define ME events in a more formal but almost identical sense, classing years as ME when the September–February Niño-3.4 is stronger than Niño-3 and Niño-4. This means that our method is fully objective and it can be applied to any dataset. This is important for our purposes as it is used in other studies with climate model output. The Niño-3.4 region (5°N–5°S, 170°–120°W) is almost identical to the 120°–150°W region used by KUG09.
2) We used the HadISST1.1 data.
3) We do not detrend the SST data.
4) We suspect the KUG09 used different periods for calculating the monthly-mean climatology. We have used the World Meteorological Organization (WMO) standard period 1961–90.
5) We have performed the classification on data for the period 1950–2011. The standard deviations of the Niño indices are calculated over this entire period.

For the common time period (1970–2005), our method and that of KUG09 give very similar lists of events. The events are listed in Table A1 from both studies. There are only two differences in the El Niño classifications: we do not classify 1990/91 as an El Niño year (of any type), and we find 2002/03 to be a ME whereas KUG09 found it to be WPE; CTE events are classified identically by the two

TABLE A1. Classification of El Niño events from 1970–2005 for this study and that of Kug et al. (2009) into the three different El Niño types.

Type	This study	KUG09
Warm pool El Niño	1977/78	1977/78
	1994/95	1990/01
		1994/95
		2002/03
	2004/05	2004/05
Mixed El Niño	1986/87	1986/87
	1987/88	1987/88
	1991/92	1991/92
	2002/03	
Cold tongue El Niño	1972/73	1972/73
	1976/77	1976/77
	1982/83	1982/83
	1997/98	1997/98

studies. KUG09's Fig. 2 shows that 1990 had the lowest standardized index of all their El Niño events, and 2002/03 had Niño-4 and Niño-3.4 values that were very similar. These small differences indicate that the exact classification is somewhat sensitive to the exact data and time periods used for calculating climatologies and trends.

We did not detrend the HadISST1.1 data, but the results do not change for most of the El Niño types. Linear detrending of the September–February Niño-3 and Niño-3.4 time series changes none of the classified CTE and ME events. However, the WPE events do change if Niño-4 is detrended. The Niño-4 has the largest linear trend from 1950–2011 of the three indices, $0.06°C\,decade^{-1}$, compared with $0.02°$ and $0.04°C\,decade^{-1}$ for Niño-3.4 and Niño-3, respectively. As the WPE events have smaller SST anomalies than the other events, these higher trends mean that the classification of WPE events is much more sensitive to detrending than the other types. Also, linear trends are very sensitive to the exact years used. From 1970 to 2005, the period used by KUG09, Niño-4 has a trend of $0.19°C\,decade^{-1}$, more than 3 times that from 1950 to 2011, and this is the 36-yr period with the highest trend during 1950–2011; the 1976–2011 trend is $-0.10°C\,decade^{-1}$. Our decision to not detrend the SST is based on this high variation of the trends due to the variability of ENSO—the trend is extremely sensitive to the exact years chosen and whether El Niño or La Niña events fall at the beginning or end of the period.

The classification of events is also sensitive to the exact years chosen for calculating climatologies and standard deviations of indices. We have used a standard period (1961–90) for climatologies. Evidently, given the general warming trend of SSTs during the past century and the high interannual and interdecadal variability of SSTs in Pacific, changing the years used will have some impact. For example, changing the climatological period

to 1971–2000 results in 1976 no longer being classed as an EPE year; using 1950–2011 changes 1994/95 from a WPE to a ME year.

The type classification used in this study and in KUG09 will always have some measure of subjectivity or dependency on the dataset used, the exact definitions, and the time periods used. This means the year classified will change. However, our study is focused on the impacts in the climate system to different ENSO events, and our classification attempts to find commonalities among almost a continuum of variations. To that end, the exact classification of individual years is of secondary relevance to the finding of robust responses to different types of events.

REFERENCES

Adler, R. F., and Coauthors, 2003: The version 2 Global Precipitation Climatology Project (GPCP) monthly precipitation analysis (1979–present). *J. Hydrometeor.,* **4,** 1147–1167, doi:10.1175/1525-7541(2003)004<1147:TVGPCP>2.0.CO;2.

Allan, R. J., R. Lindesay, and D. Parker, 1996: *El Niño Southern Oscillation and Climatic Variability*. CSIRO, 402 pp.

Ashok, K., S. K. Behera, S. A. Rao, H. Weng, and T. Yamagata, 2007: El Niño Modoki and its possible teleconnection. *J. Geophys. Res.,* **112,** C11007, doi:10.1029/2006JC003798.

Brown, J. R., S. B. Power, F. P. Delage, R. A. Colman, A. F. Moise, and B. F. Murphy, 2011: Evaluation of the South Pacific convergence zone in IPCC AR4 climate model simulations of the 20th century. *J. Climate,* **24,** 1565–1582, doi:10.1175/2010JCLI3942.1.

Cai, W., and T. Cowan, 2009: La Niña Modoki impacts Australia autumn rainfall variability. *Geophys. Res. Lett.,* **36,** L12805, doi:10.1029/2009GL037885.

——, and Coauthors, 2012: More extreme swings of the South Pacific convergence zone due to greenhouse warming. *Nature,* **488,** 365–369, doi:10.1038/nature11358.

Cambers, G., K. Hennessy, and S. Power, Eds., 2011: *Regional Overview*. Vol. 1, *Climate Change in the Pacific: Scientific Assessment and New Research,* CSIRO, 257 pp.

Chung, C. T. Y., S. B. Power, J. M. Arblaster, H. A. Rashid, and G. Roff, 2014: Nonlinear precipitation response to El Nino and global warming in the Indo-Pacific. *Climate Dyn.,* **42,** 1837–1856, doi:10.1007/s00382-013-1892-8.

Collins, D., A. Sen Gupta, and S. Power, 2011: Observed climate variability and trends. *Regional Overview,* Vol. 1, *Climate Change in the Pacific: Scientific Assessment and New Research,* G. Cambers, K. Hennessy, and S. Power, Eds., CSIRO, 51–77.

Dee, D. P., and Coauthors, 2011: The ERA-Interim reanalysis: Configuration and performance of the data assimilation system. *Quart. J. Roy. Meteor. Soc.,* **137,** 553–597, doi:10.1002/qj.828.

Folland, C. K., J. A. Renwick, M. J. Salinger, and A. B. Mullan, 2002: Relative influences of the interdecadal Pacific oscillation and ENSO on the South Pacific convergence zone. *Geophys. Res. Lett.,* **29** (13), doi:10.1029/2001GL014201.

Gray, W. M., 1979: Hurricanes: Their formation structure and likely role in tropical circulation. *Meteorology over the Tropical Oceans,* D. B. Shaw, Ed., Royal Meteorological Society, 155–218.

Griffiths, G. M., M. J. Salinger, and I. Leleu, 2003: Trends in extreme daily rainfall across the South Pacific and relationship to the South Pacific convergence zone. *Int. J. Climatol.,* **23,** 847–869, doi:10.1002/joc.923.

Hoerling, M., A. Kumar, J. Eischeid, and B. Jha, 2008: What is causing the variability in global mean land temperature? *Geophys. Res. Lett.,* **35,** L23712, doi:10.1029/2008GL035984.

Irving, D., and Coauthors, 2011: Evaluating global climate models for the Pacific island region. *Climate Res.,* **49,** 169–187, doi:10.3354/cr01028.

Jones, D. A., and Coauthors, 2012: An updated analysis of homogeneous temperature trends at Pacific Island stations. *Aust. Meteor. Oceanogr. J.,* **63,** 285–302.

Kao, H.-Y., and J.-Y. Yu, 2009: Contrasting eastern-Pacific and central-Pacific types of El Niño. *J. Climate,* **22,** 615–632, doi:10.1175/2008JCLI2309.1.

Kug, J.-S., F. F. Jin, and S.-I. An, 2009: Two types of El Niño events: Cold tongue El Niño and warm pool El Niño. *J. Climate,* **22,** 1499–1515, doi:10.1175/2008JCLI2624.1.

——, J. Choi, S.-I. An, F. F. Jin, and A. T. Wittenberg, 2010: Warm pool and cold tongue El Niño events as simulated by the GFDL 2.1 Coupled GCM. *J. Climate,* **23,** 1226–1239, doi:10.1175/2009JCLI3293.1.

Larkin, N. K., and D. E. Harrison, 2005: Global seasonal temperature and precipitation anomalies during El Niño autumn and winter. *Geophys. Res. Lett.,* **32,** L13705, doi:10.1029/2005GL022738.

Lee, T., and M. J. McPhaden, 2010: Increasing intensity of El Niño in the central-equatorial Pacific. *Geophys. Res. Lett.,* **37,** L14603, doi:10.1029/2010GL044007.

Lengaigne, M., and G. A. Vecchi, 2009: Contrasting the termination of moderate and extreme El Niño events in coupled general circulation models. *Climate Dyn.,* **35,** 299–313, doi:10.1007/s00382-009-0562-3.

McBride, J. L., and N. Nicholls, 1983: Seasonal relationship between Australian rainfall and the Southern Oscillation. *Mon. Wea. Rev.,* **111,** 1998–2004, doi:10.1175/1520-0493(1983)111<1998:SRBARA>2.0.CO;2.

McGregor, S., A. Timermann, N. Schneider, M. F. Stuecker, and M. H. England, 2012: The effect of the South Pacific convergence zone on the termination of El Niño events and the meridional asymmetry of ENSO. *J. Climate,* **25,** 5566–5586, doi:10.1175/JCLI-D-11-00332.1.

McPhaden, M. J., S. E. Zebiak, and M. H. Glantz, 2006: ENSO as an integrating concept in the earth sciences. *Science,* **314,** 1740–1745, doi:10.1126/science.1132588.

——, T. Lee, and D. McClurg, 2011: El Niño and its relationship to changing background conditions in the tropical Pacific Ocean. *Geophys. Res. Lett.,* **38,** L15709, doi:10.1029/2011GL048275.

Murphy, B., A. Sen Gupta, and S. McGree, 2011: Climate of the western Pacific and East Timor. *Regional Overview,* Vol. 1, *Climate Change in the Pacific: Scientific Assessment and New Research,* G. Cambers, K. Hennessy, and S. Power, Eds., CSIRO, 23–49.

Philander, S. G., 1990: *El Niño, La Niña, and the Southern Oscillation*. Academic Press, 293 pp.

Power, S. B., and I. N. Smith, 2007: Weakening of the Walker circulation and apparent dominance of El Nino both reach record levels, but has ENSO really changed? *Geophys. Res. Lett.,* **34,** L18702, doi:10.1029/2007GL030854.

——, and G. Kociuba, 2012: The impact of global warming on the Southern Oscillation Index. *Climate Dyn.,* **37,** 1745–1754, doi:10.1007/s00382-010-0951-7.

——, F. Tseitkin, S. J. Torok, B. Lavery, R. Dahni, and B. McAvaney, 1998: Australian temperature, Australian rainfall and the

Southern Oscillation, 1910–1992: Coherent variability and recent changes. *Aust. Meteor. Mag.,* **47,** 85–101.

——, T. Casey, C. Folland, A. Colman, and V. Mehta, 1999: Interdecadal modulation of the impact of ENSO on Australia. *Climate Dyn.,* **15,** 319–324, doi:10.1007/s003820050284.

——, A. Schiller, G. Cambers, D. Jones, and K. Hennessy, 2011: The Pacific Climate Change Science Program. *Bull. Amer. Meteor. Soc.,* **92,** 1409–1411, doi:10.1175/BAMS-D-10-05001.1.

Rayner, N. A., D. E. Parker, E. B. Horton, C. K. Folland, L. V. Alexander, and D. P. Rowell, E. C. Kent, and A. Kaplan, 2003: Global analyses of sea surface temperature, sea ice, and night marine air temperature since the late nineteenth century. *J. Geophys. Res.,* **108,** 4407, doi:10.1029/2002JD002670.

Ropelewski, C. F., and M. S. Halpert, 1989: Precipitation patterns associated with the high index phase of the Southern Oscillation. *J. Climate,* **2,** 268–284, doi:10.1175/1520-0442(1989)002<0268:PPAWTH>2.0.CO;2.

Smith, T. M., and R. W. Reynolds, 2004: Improved extended reconstruction of SST (1854–1997). *J. Climate,* **17,** 2466–2477, doi:10.1175/1520-0442(2004)017<2466:IEROS>2.0.CO;2.

Takahashi, K., A. Montecinos, K. Goubanova, and B. Dewitte, 2011: ENSO regimes: Reinterpreting the canonical and Modoki El Niño. *Geophys. Res. Lett.,* **38,** L10704, doi:10.1029/2011GL047364.

Tokinaga, H., S.-P. Xie, A. Timmermann, S. McGregor, T. Ogata, H. Kubota, and Y. M. Okumura, 2012: Regional patterns of tropical Indo-Pacific climate change: Evidence of the Walker circulation weakening. *J. Climate,* **25,** 1689–1710, doi:10.1175/JCLI-D-11-00263.1.

Trenberth, K. E., 1976: Spatial and temporal variations of Southern Oscillation. *Quart. J. Roy. Meteor. Soc.,* **102,** 639–653, doi:10.1002/qj.49710243310.

——, and Coauthors, 2007: Observations: Surface and atmospheric climate change. *Climate Change 2007: The Physical Science Basis,* S. Solomon et al., Eds., Cambridge University Press, 235–336.

Vincent, D. G., 1994: The South Pacific convergence zone (SPCZ): A review. *Mon. Wea. Rev.,* **122,** 1949–1970, doi:10.1175/1520-0493(1994)122<1949:TSPCZA>2.0.CO;2.

Vincent, E. M., M. Lengaigne, C. E. Menkes, N. C. Jourdain, P. Marchesiello, and G. Madec, 2011: Interannual variability of the South Pacific convergence zone and implications for tropical cyclone genesis. *Climate Dyn.,* **36,** 1881–1896, doi:10.1007/s00382-009-0716-3.

Wang, G., and H. H. Hendon, 2007: Sensitivity of Australian rainfall to inter-El Niño variations. *J. Climate,* **20,** 4211–4226, doi:10.1175/JCLI4228.1.

Yeh, S.-W., J.-S. Kug, B. Dewitte, M.-H. Kwon, B. P. Kirtman, and F.-F. Jin, 2009: El Nino in a changing climate. *Nature,* **461,** 511–514, doi:10.1038/nature08316.

——, B. P. Kirtman, J.-S. Kug, W. Park, and M. Latif, 2011: Natural variability of the central Pacific El Niño event on multi-centennial timescales. *Geophys. Res. Lett.,* **38,** L02704, doi:10.1029/2010GL045886.